Biotechnology Reports 29 (2021) e00585

Contents lists available at ScienceDirect

Biotechnology Reports

journal homepage: www.elsevier.com/locate/btre

Impact of nanoparticle inclusion on bioethanol production process kinetic and inhibitor profile

Isaac A. Sanusi[a,*], Terence N. Suinyuy[b], Gueguim E.B. Kana[a]

[a] Discipline of Microbiology, Biotechnology Cluster, University of KwaZulu-Natal, Pietermaritzburg Campus, South Africa
[b] School of Biology and Environmental Sciences, University of Mpumalanga, Mbombela, South Africa

ARTICLE INFO

Article history:
Received 3 October 2020
Received in revised form 8 December 2020
Accepted 31 December 2020

Keywords:
Band energy gap
Inhibitor profile
Nanoparticles
Bioethanol
Saccharomyces cerevisiae

ABSTRACT

This study examines the effects of nanoparticle inclusion in instantaneous saccharification and fermentation (NIISF) of waste potato peels. The effect of nanoparticle inclusion on the fermentation process was investigated at different stages which were: pre-treatment, liquefaction, saccharification and fermentation. Inclusion of NiO NPs at the pre-treatment stage gave a 1.60-fold increase and 2.10-fold reduction in bioethanol and acetic acid concentration respectively. Kinetic data on the bioethanol production fit the modified Gompertz model ($R^2 > 0.98$). The lowest production lag time (t_L) of 1.56 h, and highest potential bioethanol concentration (P_m) of 32 g/L were achieved with NiO NPs inclusion at different process stages; the liquefaction stage and the pre-treatment phase, respectively. Elevated bioethanol yield, coupled with substantial reduction in process inhibitors in the NIISF processes, demonstrated the significance of point of nanobiocatalysts inclusion for the scale-up development of bioethanol production from potato peels.

1. Introduction

Diminishing fossil resources, in combination with environmental pollution associated with the exploitation of these resources, make it imperative that a transition to bio-based resources is considered [1]. The utilisation of lignocellulosic biomass is desirable both for economic and environmental reasons, as substrate suitability is one of the main cost factors taken into consideration in large scale bioethanol production. It is, therefore, crucial that ethanol production is carried out using inexpensive and carbohydrate-rich feedstocks [2]. Agricultural waste is the most abundant bioresource available for use as a feedstock for biofuel production, thereby contributing to the reduction of production costs [1]. Different techniques are employed for the production of bioethanol from various bioresources (crops and lignocellulosic) depending on the geographical location, crop and the lignocellulosic biomass availability [3,4]. Potatoes (*Solanum tuberosum*) are the single most prominent vegetable crop in South Africa as the country is the number four producer of potatoes in Africa, producing an estimated 2.3×10^6 tonnes of potatoes, with the top three producing countries being Algeria (4.9×10^6), Egypt (4.8×10^6) and Malawi (4.3×10^6) [5]. Potatoes are also a staple crop across the world, currently, they became the world's fourth-largest food crop after maize, wheat, and rice [6]. The amount of potatoes processed is increasing yearly due to the expansion in the fast-food industry, increase in average income of the populace, increasing urbanisation and the inflow of international investment through international processing companies [5]. This rise in production and processing often leads to an increased generation of large volumes of waste residues such as peels, usually making up between 20–50 % of the entire tuber [6]. Most of the plant is, therefore, underutilised and its disposal has led to environmental concerns [7]. It is, therefore, necessary that an integrated, environmentally friendly solution is identified and developed [8,9].

Potato peels are a starchy, lignocellulosic waste containing intricate structures composed of lignin, hemicellulose and cellulose [10]. This food waste has been reported as one of the sustainable and foremost feedstocks for biofuel production [6]. It is

Abbreviations: NPs, Nanoparticles; wt%, Weight percent; SATP, Soaking assisted thermal pre-treatment; ISF, Instant saccharification and fermentation; SNLISF, SATP + Nano + Liquefaction + ISF; SLNISF, SATP + Liquefaction + Nano + ISF; SLISF, SATP + Liquefaction + ISF; NSLISF, Nano + SATP + liquefaction + ISF; SLIS, SATP + Liquefaction + SS + No Fermentation; NSLIS, Nano + SATP + Liquefaction + SS + No Fermentation; HMF, 5-Hydroxymethyl Furfural; ORP, Oxidation–reduction potential; ATP, Adenosine triphosphate; VICs, Volatile inhibitory compounds; SPR, Surface plasmon resonance; SPA, Surface Plasmon Absorption; UV–vis, Ultraviolent visible; TEM, Transmission electron microscopy; SEM, Scanning electron microscopy; EDX, Energy-dispersive X-ray spectroscopy; EDS, Energy dispersive spectrophotometric; GC–MS, Gas chromatography-Mass spectrometry.

* Corresponding author.
E-mail addresses: Sanusi_isaac@yahoo.com, SanusiA@ukzn.ac.za (I.A. Sanusi).

https://doi.org/10.1016/j.btre.2021.e00585

currently receiving great interest as its bioconversion to high-value products such as renewable fuels do not directly compete with food security [11]. The potential of waste potato material as a feedstock for bioethanol production has recorded some successes [12–14]. For instance, Fadel [15] achieved high alcohol concentration of 13.2 % *v*/*v* in a fermentation broth containing 25 % *w*/*v* glucose from potato waste. Likewise, Arapoglou et al. [8] obtained 18.5 g/L fermentable sugar from the enzymatic hydrolysis of potato peel waste with a group of three enzymes and produced 7.6 g/L of ethanol after fermentation. Efforts towards the use of starch-based lignocellulosic biomasses for bioethanol production are being challenged by low sugar yield from substrate, high inhibitor production, high production cost and low fermentation efficiency [16], thus highlighting the need for further optimisation.

Despite the vast information available on the use of pre-treated starch-based substrate for bioethanol production, there is a dearth of literature on the kinetics of *Saccharomyces cerevisiae* growth and bioethanol production from potato peels under nanobiocatalyst conditions. Studies on kinetics would provide insights into the impact of process parameters on bioethanol formation [17,18]. Moreover, kinetic modelling can be used to predict the dynamics of substrate utilisation and bioethanol production rate. Usually, these models are employed to improve the yield and the productivity of high-quality product. The release of detrimental and inhibitory can also be minimised using these models [19]. The modified Gompertz model is employed to evaluate production lag time, maximum product production rate, and maximum product concentration on a given substrate [20]. Such model could provide valuable process products knowledge on bioethanol production process using potato peels as feedstock in the presence of a nanobiocatalyst.

Nano-size materials have attracted huge interest for their unique material properties and their corresponding practical applications in biotechnology [21,22] Nanoparticles (NPs) have been used extensively in biomedicine, drug delivery, biosensors, water purification and environmental remediation [21,23]. Some biological applications include immobilisation of enzymes, microbial cells, as well as biocatalytic agents [23,24]. The strategy of using nanobiocatalytic agents in bioprocesses is to increase process efficiency through increased mass and heat transfer, enzymatic and cell metabolic activities arising from their large surface areas, catalytic properties, growth and enzyme cofactor functionality [25,26]. Besides their importance as cofactor for enzymatic activities, they are also required to aid the structural stability of several proteins and enzymes, many could exert significant control on cellular metabolic processes and ultimately process performance [27]. Furthermore, nano-compounds such as NiO and Fe_3O_4 provide a suitable start-up environment for bioproduct formation due to their ability to modulate oxidation-reduction potential (ORP) values [28]. Yet, the application of this approach is limited because of the poor understanding of the process and the limited available information on nanocatalysed bioethanol fermentation.

Process conditions used for the pre-treatment of lignocellulosic biomass result in the formation of inhibitory compounds [29]. The negative impact of these inhibitors are usually longer microbial lag time and lower cell concentration. In addition, many of these compounds have been reported to influence negatively enzymatic hydrolysis and fermentation processes. Fermentation inhibitors include aliphatic acids, ketones, phenolic compounds, furan-derivatives and alcohols [30]. Their concentrations differ, depending on the structure of the lignocellulosic biomass employed and the pre-treatment techniques implemented [29,30]. Knowledge of profile of inhibitory compounds from various stages of biomass conversion, namely, pretreatment, liquefaction, saccharification and fermentation in the presence of nanocatalyts would enhance the understanding of the interaction of the biomass and nanoparticles.

The primary biological technique for the production of bioethanol from lignocellulosic feedstock is the instantaneous saccharification and fermentation process. During this process lignocellulosic feedstock is first saccharified by hydrolytic processes to release fermentable sugar, which is simultaneously fermented to produce bioethanol [26]. In instantaneous saccharification and fermentation (ISF), the overall process is limited by the need to optimise enzymatic and cellular activities for maximum sugar release and subsequent ethanol formation as well as to minimise inhibitor formation during the pre-treatment and fermentation processes [16]. Recent studies have examined parameter optimisation as a technique to improve the efficiency of instantaneous saccharification and fermentation process [31,16]. Attempts to include nanoparticles as biocatalytic agents to enhance heat and mass transfer rates, buffering capacity, enzymatic activities and cellular functionality continue to attract great interest [23,24,26,32,33]. Very little is known on the instantaneous saccharification and fermentation process with nanobiocatalyst inclusion at various process namely, liquefaction and pre-treatment stages.

This study therefore examines the impact of nanoparticle inclusion at different stages of ISF, using waste potato peels as substrate and to model the bioethanol production using the modified Gompertz model. In addition, the effect of nanoparticle inclusion on the process volatile compounds profile was also evaluated.

2. Materials and methodologies

2.1. Potato peel powder preparation

Potato peels were collected from food vendors in the Pietermaritzburg metropolis, KwaZulu-Natal province, South Africa. They were immediately oven-dried at 50−55 °C and milled to 1−2 mm particle size using a centrifugal miller. Composition analysis [34] of pulverised waste potato peels show 20 % starch, 14 % structural carbohydrate, 4 % cellulose, 10 % hemicellulose, 6 % lignin and 46 % others (lipids, protein, moisture content and ash contents).

2.2. Soaking assisted thermal pre-treatment (SATP)

The powdered waste potato peels (Fig. 1) were subjected to previously optimised process parameters of pre-treatment [35]. Briefly, 0.92 % (v/v) HCl solution at a solid-to-liquid (S:L) ratio of 10 % solid loading was soaked in a water bath without shaking for 2.34 h at 69.6 °C and followed by 5 min autoclave treatment (121 °C). The pH of the treated potato peel biomass was thereafter brought to neutrality in preparation for the enzymatic hydrolysis (the

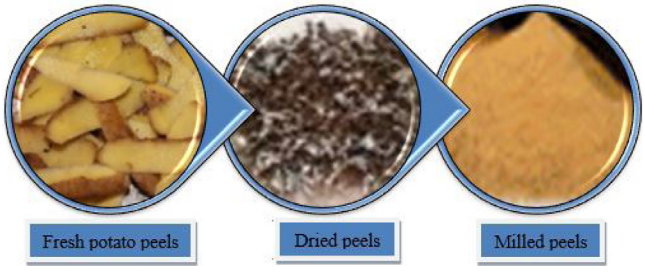

Fig. 1. Flowchart of SATP pulverised waste potato peels.

hydrolytic enzymes-amylase and amyloglucosidase used were purchased from Sigma-Aldrich, South Africa).

2.3. Microorganism and inoculum preparation

An Erlenmeyer flask containing 100 mL Yeast-Peptone-Dextrose broth was inoculated with *S. cerevisiae* BY4743 and grown at 120 rpm, 30 °C overnight, to attain an exponential growth phase. This cultivation was subsequently used as seed-culture (10 %) source for the instantaneous saccharification and fermentation.

2.4. Preparation of nanomaterials

NiO nanoparticles (NPs) were synthesised by dissolving an appropriate amount of $NiCl_2.6H_2O$ in distilled water. Then NH_3 solution is added dropwise to reach a pH of 10. The solution was treated with microwave irradiation operated at a power of 700 W for 180 s, and the culmination of the reaction was signalled by the precipitation of light green NiO NPs. The NiO nanoparticle obtained were washed a few times with deionized water and oven dried for six hours [24].

Iron (III) oxide nanoparticles (Fe_3O_4 NPs) were synthesised by dissolving 1.0 g of $FeSO_4.7H_2O$ in distilled water, and the pH was adjusted to 12, then the volume was made up to 200 mL. The solution was heated in a microwave oven at 700 W for 600 s. The obtained black magnetic Fe_3O_4 NPs precipitate was rinsed a few times and dried at 70 °C for a couple of hours [36].

2.5. Characterisation of nanoparticles

The morphology of NiO and Fe_3O_4 NPs was determined by a scanning electron microscope (SEM, ZEISS-EVO/LS15, ZEISS instrument, Germany). Each sample was mounted on an aluminium grid coated with carbon prior to scanning electron microscopy (SEM) analysis. Transmission electron microscopy (TEM) was used to study the shape and the particle size of the NPs. TEM image was captured on JEM-1400 electron microscope operating at 120 kV. The ultra-violet visible (UV–vis) absorption spectral properties of the nanoparticles were investigated by absorption spectroscopy using an ultra-violet visible spectrophotometry (200−700 nm).

2.6. Nanoparticle inclusion in instantaneous saccharification-fermentation (NIISF)

The NIISF experiments were carried out using hydrolysate from the SATP [32] pre-treatment stage. The NIISF process (50 mL) contained pulverised and pre-treated potato peels; 10 % solid loading, 0.212 mL liquefying amylase (at 90 °C, pH 7, for an hour), 0.295 mL saccharifying amyloglucosidase and fermentation nutrients: yeast extract-5 g/L, KH_2PO_4-2 g/L, $MgSO_4$-1 g/L, $(NH_4)_2SO_4$-1 g/L. *S. cerevisiae* inoculum (10 %) was introduced, then, the different NIISF set-up in replicates were incubated at 37 °C and 120 rpm over 24 h until glucose concentrations were depleted. Aliquot of 0.5 mL were extracted at regular interval for sample analysis. The NIISF designs [24] with nanoparticle supplementation at various process stages are shown below (Fig. 2).

2.7. Analytical methods

2.7.1. Glucose, bioethanol and cell concentration determination

The glucose concentration in the sampled aliquot was determined using D-glucose Assay Kit (Megazyme, Ireland).

The amount of bioethanol produced was determined using a bioethanol vapour sensor (LABQUEST®2, Vernier, USA) [24].

2.7.2. Kinetic model constants

The bioethanol empirical data were used to fit the modified Gompertz model. The model Eq. (4) is shown below.

$$P = P_m \ .\exp\left\{-\exp\frac{r_{p.m} \ .\exp(1)}{P_m}.\ (t_L - t) + 1\right\} \quad (4)$$

where P is the bioethanol concentration, (g/L), P_m is the potential maximum bioethanol concentration, (g/L), $r_{p.m}$ is the maximum bioethanol production rate (g/L/h) and t_L is the lag time of bioethanol production (h).

2.7.3. Calculation of bioethanol yield (wt.%) and bioethanol productivity (g/L/h)

Glucose utilisation, fermentation efficiency, bioethanol yield and bioethanol productivity were obtained using the following

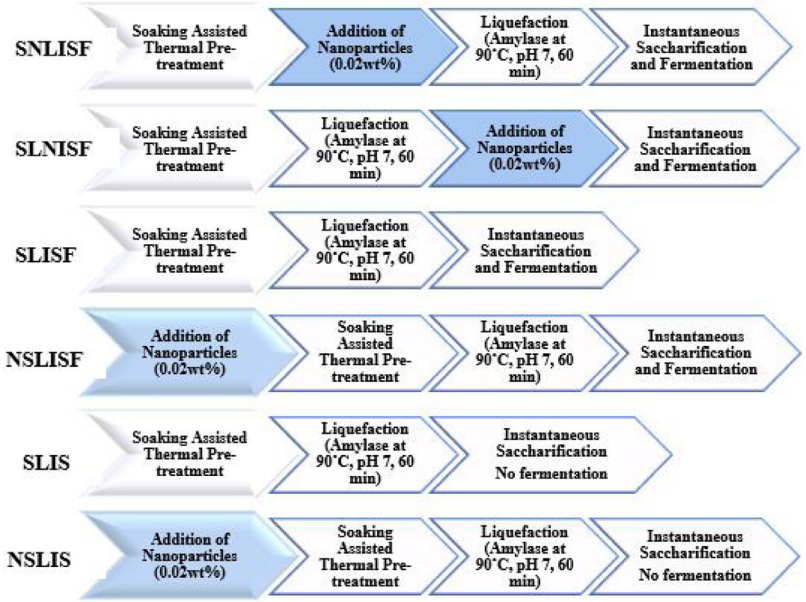

Fig. 2. Process flow diagram showing stages of nanoparticle inclusion in the ISF process. Nanoparticles (0.02 wt.% relative to biomass weight) were added at the pre-treatment (NSLISF), the liquefaction (SNLISF) and the saccharification (SLNISF) stages. The control is without nanoparticle inclusion (SLIS).

Eqs. (5)–(7) respectively.

$$Sugar\ utilisation\ (\%) = \frac{Initial\ sugar\ content - final\ sugar\ content}{Initial\ sugar\ content} \times 100 \quad (5)$$

$$Ethanol\ yield\ (g/g) = \frac{Maximum\ ethanol\ concentration\ (g/L)}{Utilized\ glucose\ (g/L)} \quad (6)$$

$$Ethanol\ productivity\ (g/L/h) \frac{Maximum\ ethanol\ concentration\ (g/L)}{Fermentation\ time\ (h)} \quad (7)$$

2.7.4. Analysis of volatile organic inhibitory compounds

Analysis of inhibitory compounds such acetic acid, furfural, 5-Hydroxymethylfufural (HMF) and ketones from the fermentation broth was carried out using with Varian 3800 gas chromatography (Varian Palo Alto, California, USA) and Varian 1200 mass spectrometry [30].

3. Results and discussion

3.1. Characterization of NiO and Fe_3O_4 nanoparticles (NPs) with SEM and TEM

In Fig. 3A, SEM-EDS analyses showed the surface morphology and elemental constituent of Fe_3O_4 nanoparticles. Strong signals corresponding to Fe (56.06 %), and oxygen (30.19 %) were observed. Other elemental constituent of Fe_3O_4nanoparticles were C (13.40 at %) and Si (0.34 at %). Similarly, the Scanning Electron micrograph showed the aggregated NiO nanoparticle, and the elemental composition obtained using the SEM-EDS machine is Ni (31.46 at %), C (35.04 at %), O (32.53 at %), Cl (0.50 at %) and Si (0.48 at %). The TEM micrograph (Fig. 4A) shows that Fe_3O_4 particles were roughly spherical with particle size in the range of 18−39 nm with a mean size of 31 nm. Equally, the TEM image of NiO nanoparticle is depicted in Fig. 4B with an average mean size of 29 nm.

Ultraviolent visible (UV) absorption spectra of NiO and FeO_4 NPs were presented in Fig. 5. The UV–vis absorptions showed sharp absorption at 220 and 282 nm due to nickel and iron oxide metal nanoparticles respectively [37]. This can be attributed to the Surface Plasmon Resonance (SPR). The SPR originates from resonance of collective conduction electrons with incident electromagnetic radiations. The frequency and width of the Surface Plasmon Absorption (SPA) usually depends on the size and shape of the nanomaterials. In addition, the dielectric constant of the metal itself and the surrounding medium influences the SPA [38]. Also, the profile of the resonance peak can be qualitatively related to the nature of the NPs. NiO NPs with a small and uniform-sized narrow distribution (23−37 nm) produces a sharp absorbance, however, Fe_3O_4NP with a larger particle size and aggregation shows a broad absorbance [37,38].

3.2. Effect of nanoparticle band gap energy on bioprocessing

From the curve in Fig. 5, the band gap energy of Fe_3O_4 NPs and NiO NPs were 4.04 eV and 4.51 eV, respectively [39]. The inclusion of NiO nanoparticle in the fermentation process resulted in better process efficiency and consequently, higher productivities when compared to Fe_3O_4 NPs supplemented fermentation process (Table 1). This impact by NiO NPs inclusion can be attributed to the size of it band energy gap which is typical of efficient catalyst [40,41]. Activation energy and NPs catalytic potentials are usually dependent on band gap energy. In other words, lower activation energy is associated with higher energy gap, such as obtained in this study. Consequently, band energy gap could impact the interaction/affinity between the nanoparticles, the yeast and the substrate [24]. The process time for nanoparticle supplemented fermentation process achieved peak ethanol production after 16 h. This was two-fold faster than the result obtained in the control experiment. This clearly indicates the presence of the nanoparticles had high catalytic effect on the biochemical processes to improve bioethanol production. This catalytic activity could also be ascribed in part to its band energy gap. Likewise, the efficiency of heat and mass transfer which are vital bioprocess conditions, could

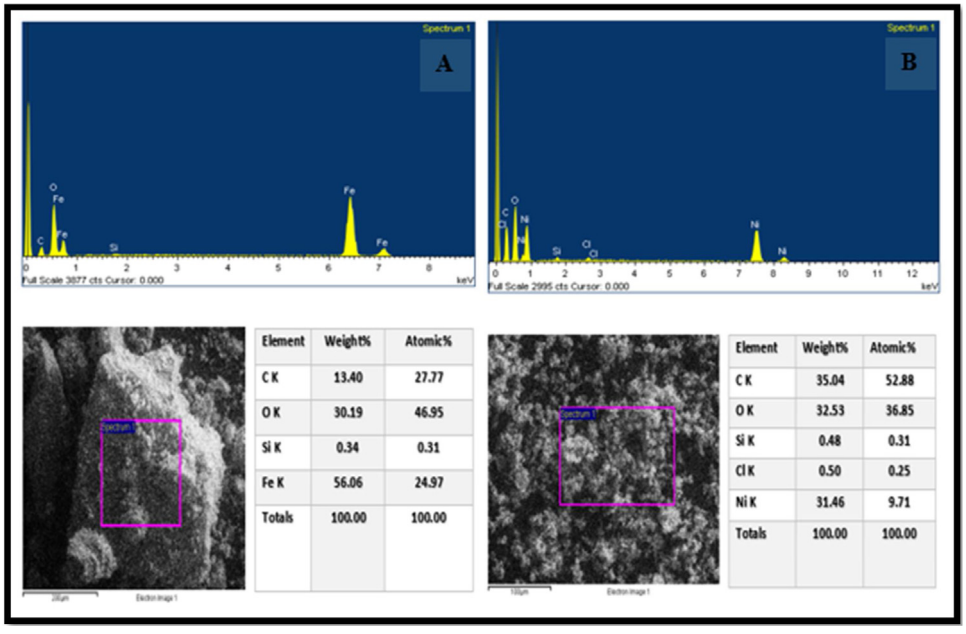

Fig. 3. Scanning electron microscopy (SEM) image and EDX Spectrum of Fe_3O_4 NPs (A) and NiO NPs (B).

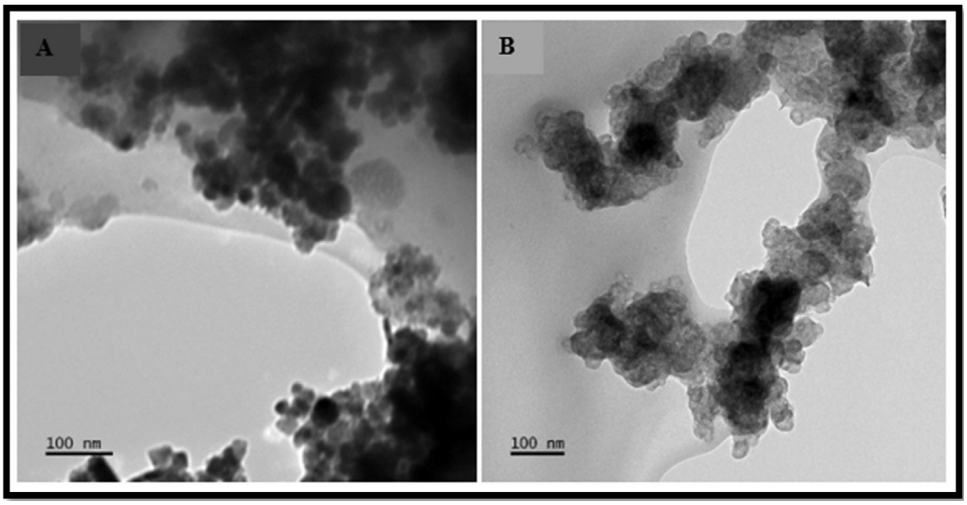

Fig. 4. Transmission electron microscopy (TEM) micrographs of Fe_3O_4 NPs (A) and NiO NPs (B) showing the shape and weak agglomeration of the nanoparticles.

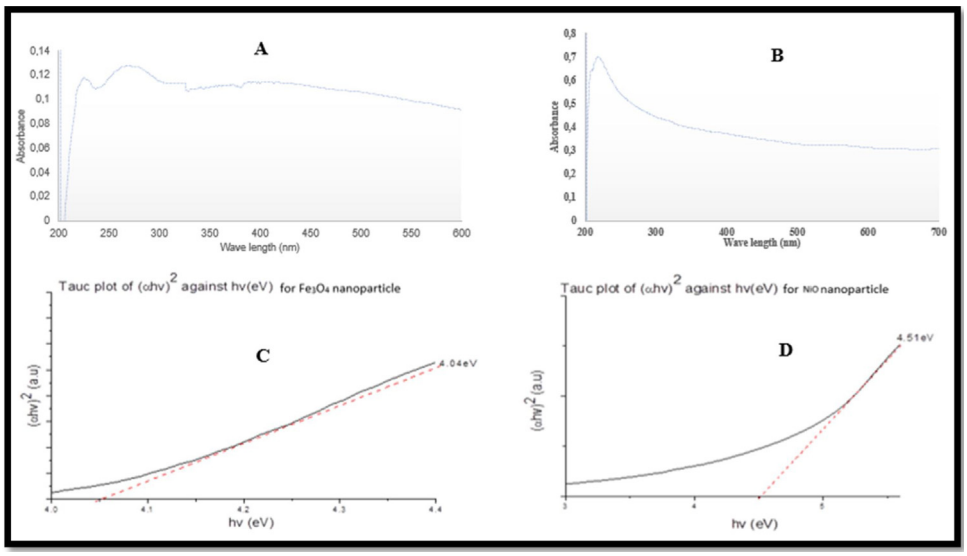

Fig. 5. Fe_3O_4 NPs (A), NiO NPs (B), Tauc plot of Fe_3O_4 NPs (C) and Tauc plot of NiO NPs (D).

Table 1
Performance of ISF processes with nanoparticle inclusion.

ISF mode with NiO NPs	SNLISF	SLNISF	SLISF (control)	NSLISF
Glucose utilization (%)	96.00	100,00	100.00	99.00
Bioethanol yield (g/g)	0.50	0.50	0.40	0.70
Bioethanol concentration (g/L)	25.85	25.63	22.53	36.04
Bioethanol productivity (g/L/h)	0.90	0.80	0.90	2.25

ISF mode with Fe_3O_4 NPs	SNLISF	SLNISF	SLISF	NSLISF
Glucose utilization (%)	97.00	100.00	100.00	96.00
Bioethanol yield (g/g)	0.93	0.60	0.46	0.79
Bioethanol concentration (g/L)	23.99	25.49	22.49	23.75
Bioethanol productivity (g/L/h)	1.99	1.60	0.90	1.98

be influenced by band gap size. Mass transfer phenomena are considered under the Poole–Frenkel effect and small-polaron mechanism: these are band energy gap dependent [40,41]. The most remarkable correlation is: the smaller the particle size, the higher the energy gap, that could occasion lower activation energy hence, high process performance. The synthesis of a nanomaterial with suitable band energy gap would enables the optimal electron transfer and catalytic properties, that could support high process performance.

3.3. Bioethanol production from potato peels

Bioethanol evolution under Fe_3O_4 NIISF (Fig. 6A) and NiO NIISF (Fig. 6B) fermentation processes revealed a short lag time (4 h) for all modes in both nano systems. The NSLISF (NiO NIISF) process showed a sharp increase in bioethanol concentration up to 36.04 g/L, the highest obtained of the NiO NIISF processes which occurred from 4 to 20 h in comparison to 25.13 g/L (Mode SLNISF), the highest of the Fe_3O_4 NIISF processes. Maximum bioethanol concentrations were obtained during the log yeast cell growth stage in the NSLISF (NiO NIISF) and SLNISF (Fe_3O_4NIISF) and were higher than the control experiment (Mode SLISF) in both systems. These were linked with precipitous utilisation of glucose by the yeast and bioethanol formation. Further increment in bioethanol concentration was not observed after the log phase, due to nutrient exhaustion besides fermentable sugar depletion. Ethanol yields of 0.48, 0.48, 0.42 and 0.71 g-ethanol/g-glucose (Table 1)

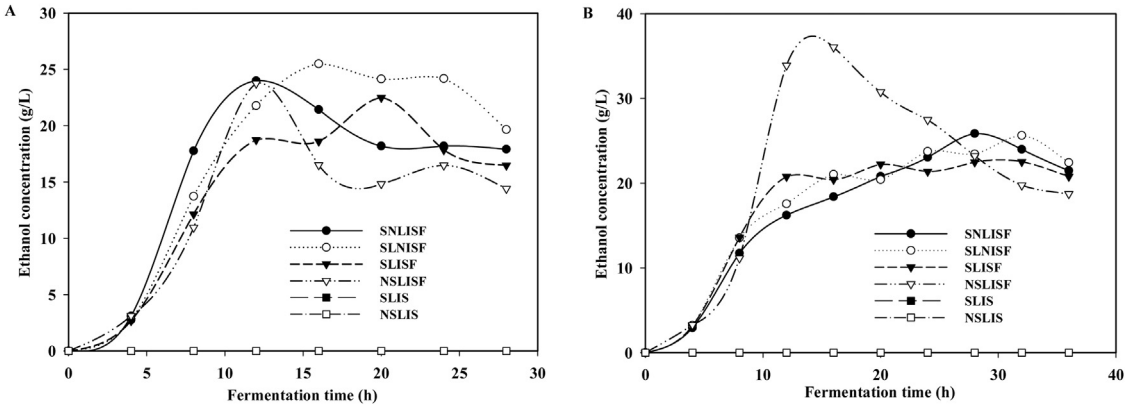

Fig. 6. Production of bioethanol as a function of fermentation time showing the impact of Fe_3O_4 NPs (A) and NiO NPs (B) inclusion.

corresponding to productivities of 0.92, 0.80, 0.92 and 2.25 g/L/h were achieved for NiO NPs ISF Mode SNLISF, SLNISF, SLISF and NSLISF respectively. Similarly, ethanol yield of 0.93, 0.58, 0.46 and 0.79 g/g was obtained, corresponding to 2.00, 1.58, 0.92 and 1.98 g/L/h productivity for Fe_3O_4 NPs ISF Mode SNLISF, SLNISF, SLISF and NSLISF respectively during the same fermentation period. The effect of NiO and Fe_3O_4 NPs inclusion on the processes were substantial. For instance, ethanol yield in the NiO NPs ISF process was 1.69-fold higher than the control set-up while a twofold (2.02-fold) increment in ethanol yield in comparison with the control set-up was observed in the Fe_3O_4 NPs ISF process. Micronutrients such as nickel and iron have a significant impact on *S. cerevisiae* growth and bioethanol formation [2,42]. Additionally, nickel oxide nanoparticles have been reported to exhibit a glucose-nanoparticle electropositive interaction [42], and this is advantageous for substrate to cell contact. Moreover, nanoparticles have stronger affinity for electrons due to their redox potential and small atomic size [43]. Strong affinity within few nanometres distance of microbes and nanoparticles under anaerobic conditions was obtained in previous reported [44]. Furthermore, the possibility of nanoparticles being adsorbed to the cell surface as well as cell adsorption to the surfaces of NPs have been reported [28,33]. Hence, improved *S. cerevisiae* substrate contact, cellular metabolism and process performance were obtained for the nano-fermentation processes [33,45,46].

In comparison, higher bioethanol concentrations were achieved with NPs inclusion in the ISF processes in relation to previous studies using potato wastes as feedstock for bioethanol production. For instance, 1.7-fold increase in the bioethanol concentration was observed in the NiO NPs ISF process compared to the study of Khawla et al. [14]. Likewise, 4.7-fold and 6.5-fold higher ethanol concentration were achieved in the NiO NPs ISF process compared to studies by Arapoglou et al. [8] and Hashem and Darwish [12], respectively. Similarly, the Fe_3O_4 NPs ISF process had higher bioethanol concentration, 25.49 g/L (4.6-fold increment), compared to previous study on potato starch residue (5.52 g/L, [12]). Again, in another related study, a 3.4-fold increase in bioethanol concentration was also obtained with the Fe_3O_4 NPs ISF process compared to the study by Arapoglou et al. [8], where the authors obtained highest bioethanol concentration of 7.6 g/L from potato peel waste using *Saccharomyces cerevisiae* var. *bayanus*. The higher bioethanol concentration in the current study is desirable and might be ascribed mainly to the nanobiocatalyst employed, which increases the chances of *S. cerevisiae* substrate contact, utilisation and ultimately, enhanced process performance.

Furthermore, the highest bioethanol productivity of 2.25 g/L/h was achieved with NiO NPs inclusion during the pre-treatment stage in the present study (Table 2). By comparison, lower ethanol productivity, in the range of 0.15 to 0.25 g/L/h from previous studies was achieved by Arapoglou et al. [8] and Khawla et al. [14], both also using potato peel as substrate. Similarly, Hashem and Darwish [12] reported ethanol productivity of 0.15 g/L/h which was 15-fold lower than the current study. Additionally, in two different studies, Izmirlioglu and Demirci [13] and Izmirlioglu and Demirci [47] reported bioethanol productivities of 0.29 and 0.27 g/L/h, respectively using waste potato mash as feedstock. The obtained productivities were 7.8-fold and 8.3-fold, respectively lower when compared to the current study. The reported variations observed in these bioethanol productivities can be attributed mainly to the presence of nano additives as well as the different potato waste feedstock, yeast strain, and the fermentation approach employed [48].

Table 2
Comparison of bioethanol productivity with previous studies.

Substrate	Yeast	Productivity (g/L/h)	References
Waste potato peels	*S. cerevisiae* BY4743	0.92	This study (NiO NP Mode SNLISF)
Waste potato peels	*S. cerevisiae* BY4743	0.80	This study (NiO NP Mode SLNISF)
Waste potato peels	*S. cerevisiae* BY4743	0.92	This study (NiO NIP Mode SLISF-control)
Waste potato peels	*S. cerevisiae* BY4743	2.25	This study (NiO NP Mode NSLISF)
Waste potato peels	*S. cerevisiae* BY4743	1.99	This study (Fe_3O_4 NP Mode SNLISF)
Waste potato peels	*S. cerevisiae* BY4743	1.59	This study (Fe_3O_4 NP Mode SLNISF)
Waste potato peels	*S. cerevisiae* BY4743	0.92	This study (Fe_3O_4 NP Mode SLISF-control)
Waste potato peels	*S. cerevisiae* BY4743	1.98	This study (Fe_3O_4 NP Mode NSLISF)
Waste potato peels	*S. cerevisiae*	0.25	[15]
Waste potato peels	*S. cerevisiae* var. *bayanus*	0.15	[9]
Waste potato peels	S. cerevisiae y-1646	0.15	[12]
Waste potato mash	*S. cerevisiae* (ATCC 24859)	0.29	[13]
Waste potato mash	*Aspergillus niger* (NRRL 330) and *S. cerevisiae* (ATCC 24859)	0.27	[45]

The maximum bioethanol yield of 0.93 g/g was achieved in the current research. This was achieved with Fe_3O_4 NPs inclusion (NIISF Mode SNLISF). Ethanol yields between 0.38 and 0.46 g/g have been reported in previous studies [8,47]. These were 2.4 and 2.0-fold lower than the ethanol yield (0.93 g/g) obtained in present study. These observations further underscore the potential of nanobiocatalyst in the fermentation of waste potato peels and other feedstock for bioethanol production [49].

The high glucose release during the pre-treatment process can be attributed to the enhanced enzymatic hydrolysis of pre-treated waste potato peels [25]. The recovery of fermentable sugars in the nano systems was observed to be slightly higher in comparison to the control experiments (Fig. 7) and this can be ascribed to increased enzyme activities under the nanobiocatalyst conditions [50–54]. In a related study, Ban and Paul [25], reported an increase in intracellular β-glucosidase (BGL) activity up to 28 % with 5 mM ZnO nanoparticle process inclusion. Furthermore, the high glucose availability for immediate utilisation by the yeast cells could promote glycolytic rates and consequently, increase ethanol production instead of cell development, which further explains the higher bioethanol concentration observed in the nano systems.

The depletion of glucose occurred from 0 to 28 h in the Fe_3O_4 NPs inclusion ISF processes (Fig. 7A). The percentage glucose utilisation of 97.00 %, 100.00 %, 100.00 % and 94.00 % were observed under the four fermentation conditions (SNLISF, SLNISF, SLISF and NSLISF, respectively). Similarly, rapid glucose depletion was observed in the NiO NPs inclusion ISF processes from 0 to 36 h (Fig. 7B). And the maximum glucose utilisation of 96.00 %, 100.00 %, 100.00 % and 99.00 % (Table 1), was observed for SNLISF, SLNISF, SLISF and NSLISF processes respectively, further suggesting the nano catalysts favoured glucose uptake and utilisation by *S. cerevisiae*.

3.4. NIISF processes bioethanol production kinetics

The observed data fitted the modified Gompertz model (R^2 value >0.98) for the ISF NiO and Fe_3O_4 NPs inclusion modes, respectively (Table 3). The modified Gompertz kinetic model is widely used for bioproduct formation study [55,56]. This model gives information on the process lag time, the maximum bioethanol production rate, and the potential maximum bioethanol concentration. The kinetic coefficients for the highest maximum potential bioethanol concentration (P_m), maximum bioethanol production rate ($r_{p.m}$), and the lowest lag time obtained in the present study were 32 g/L, 4.50 g/L/h, and 1.56 h, obtained for the ISF NPs inclusion processes, NSLISF (NiO NPs inclusion), SNLISF (Fe_3O_4 NPs inclusion) and SNLISF (NiO NPs inclusion), respectively. All the NIISF results suggest that the presence of these nanomaterials effectively improved the bioactivity of *S. cerevisiae* and subsequently increase the formation and yield of ethanol from glucose. Also, these metals are bio-active agents such as cofactor enzymes stabilizer and activators that enhance anaerobic bioethanol fermentation [57]. Besides their role as growth factors and enzyme cofactors, they are important in stimulating the formation of cytochromes and ferroxins (Fd) which are vital for cell energy metabolism [42]. Furthermore, NPs have been reported to modulate the oxidation-reduction potential (ORP) values in bioprocessing [28]. Low ORP value enhances bioprocessing, by providing a suitable process environment for bioproduct formation such as bioethanol production [28].

Table 3 shows the comparison of modified Gompertz coefficients obtained in this study with previous studies. In the present study, maximum bioethanol production of 31.84 g/L obtained was 2.77-fold higher compared to the report by [58] and 1.5-fold higher than that achieved by [17]. Similarly, the maximum bioethanol production rate of 4.50 g/L/h was 18.75 times, 8.65 times and 1.03 times that achieved by [58] from oil palm frond juice, Rorke and Gueguim Kana [59] from sorghum leaves and Dodic et al. [19] from sugar beet raw juice, respectively. The highest P_m and $r_{p.m}$ observed in the present work coincided with NPs' presence. This further highlighted the potential of nanoparticles as efficient biocatalyst for starch-base lignocellulosic bioethanol production from ISF processes.

3.5. GC–MS volatile organic inhibitory profile

Fig. 5 shows the profile of obtained volatile organic inhibitory compounds (VOIcs) under the various modes of nano inclusion during instantaneous saccharification and fermentation (NIISF) of potato peels. Major VOIcs groups found were organic acids, alkanols and ketones. Lower fractions of aldehydes, benzenoids, sulphur-compounds, phenolic compounds, alkanals, amines and amides were also found. Frequently reported volatile inhibitory groups in bioprocessing include aliphatic acid, alcohol, aldehydes, benzenoids, phenolic compounds and ketones [28,30]. Table 4 represents the VOIcs distribution observed under different NIISF designs. The largest VOIcs part obtained was the aliphatic acids (69 %), with acetic acid making a large part (94 %), corresponding to a concentration of 16.07 g/L (Table 4). The formation of acetic acids has been reported in the pre-treatment of starch-based lignocellulosic biomass due to the release of acetate (acetyl groups of hemicelluloses) upon hemicellulose hydrolysis and fermentation of hexose sugars [35]. Acetic acid within the neutral cell environment dissociates and leads to a decline in pH which consequently impedes cellular activities. Therefore, before proceeding to fermentation, it is important that acid is neutralised,

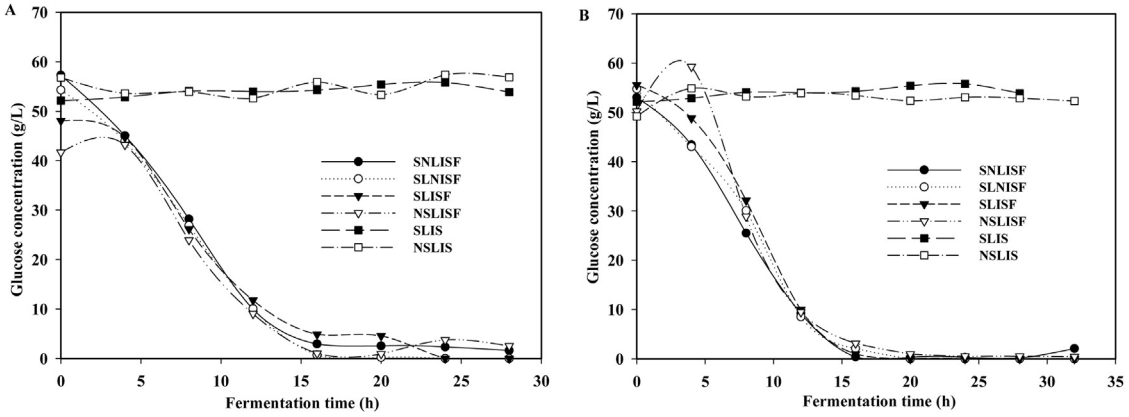

Fig. 7. Effect of inclusion of NPs on glucose utilisation during fermentation process; Fe_3O_4 NPs (A) NiO NPs (B).

Table 3
Modified Gompertz model process parameters for NIISF processes compared to previous studies.

Feedstock	P_m (g/L)	$r_{p,m}$ (g/L/h)	t_L (h)	Reference
Waste potato peels	24.64	1.56	1.56	This study (NiO NP Mode SNLISF)
Waste potato peels	24.17	1.90	1.79	This study (NiO NP Mode SLNISF)
Waste potato peels	21.85	3.02	3.18	This study (NiO NIP Mode SLISF-control)
Waste potato peels	31.84			This study (NiO NP Mode NSLISF)
Waste potato peels	23.24	4.50	3.47	This study (Fe_3O_4 NP Mode SNLISF)
Waste potato peels	24.83	3.26	3.59	This study (Fe_3O_4 NP Mode SLNISF)
Waste potato peels	22.35	2.30	2.86	This study (Fe_3O_4 NP Mode SLISF-control)
Waste potato peels	23.59			This study (Fe_3O_4 NP Mode NSLISF)
Beet raw juice	73.30	4.40	1.00	[20]
Sweet sorghum Juice	88.48	2.17	2.98	[21]
Waste sorghum leaves	17.15	0.52	6.31	[49]
Oil palm frond juice (10–20 years)	3.79	0.08	0.77	[48]
Oil palm frond juice (3–4 years)	11.50	0.24	0.12	[48]
Corn cobs waste	42.24	2.39	1.98	[17]
Corn cobs waste	32.09	3.25	2.68	[17]
Corn cobs waste	37.87	2.14	2.66	[17]
Corn cobs waste	27.62	2.33	3.12	[17]

while during fermentation metabolic shift away from acid formation will favour ethanol production [28]. Other aliphatic acids produced were, among others, propanoic acid (<0.17 g/L), isobutyric acid (<0.13 g/L), larixinic acid (<0.20 g/L) formic acid (<0.15 g/L), sorbic acid (<0.20 g/L), hexanoic acid (<0.10 g/L) and levulinic acid (<0.16 g/L). Aliphatic acids such as levulinic acid and formic acid are typically formed upon the degradation of 5-hydroxymethylfufural and furfural. It has been reported that the presence of these acids affects process performance by reduction of biomass formation and consequent inhibition of ethanol production. This occurs when less ATP is available for biomass formation resulting from intracellular build-up of anions within the fermentative microbes due to dissociation of these acids [30].

The next largest volatile fraction were the ketones, amounting to a maximum of 47 %, with 2,3-dihydro-3,5-dihydroxy-6-methyl-4H-Pyran-4-one being the most prominent, up to 93 % (4.65 g/L). Usually, 2,3-dihydro-3,5-dihydroxy-6-methyl-4H-Pyran-4-one is formed from the intermediate product of Maillard reaction of dextrose, maltose and hexoses such as glucose [60]. Other ketones formed include 1-hydroxy-2-propanone (<2.48 %), 2-Pyrrolidinone (<2.16 %), ethenone (<8.33 %) and 2,5-Dimethyl-4-hydroxy-3 (2 H)-furanone (<16.98 %), corresponding to concentrations of 0.21, 0.07, 0.27 and 0.55 g/L respectively. Generally, the formation of ketones occurs due to pentose sugars such as xylose degradation. Similarly, ketones are degradation compounds formed during lignocellulosic biomass pre-treatment and subsequently ethanol fermentation. Like other volatile compounds they have inhibitory effect on enzymes and yeast activities [61].

Phenolics such as 2-methoxy phenol and 2-methoxy-4-vinyl-phenol observed in this study were formed due to partial degradation of lignin [1]. Phenolic compounds formation can also be due to degradation or protonation of carbohydrates such as D-glucose, D-xylose and L-arabinose [61]. These phenolic compounds impede enzymatic saccharification and can lead to the destruction of cellular electrochemical gradients [30].

Other groups found were aldehydes, amines, amides, lactones, sulphur-containing compounds and alkanal fractions (Table 4). Aldehydes, mainly furfural, 5-Methyl-fufural and 5-Hydroxymethylfufural (HMF) were detected, which were products of xylose protonation that occurs at elevated pre-treatment conditions [61]. Inhibitory mechanisms of furfural and HMF in bioprocesses include furfuryl alcohol from yeast metabolism of furfural that inhibits anaerobic growth of *S. cerevisiae* and subsequently impedes ethanol production. Similarly, *S. cerevisiae* metabolises HMF to 5-hydroxymethyl furfuryl alcohol, resulting in a prolonged lag phase in microbial growth.

Furthermore, as shown in Fig. 8, aliphatic acids concentration (up to 69 %), was observed to be higher in the control experiment (Mode SLISF) compared to the NiO nano systems: Mode SNLISF (59 %), Mode SLNISF (62 %) and Mode NSLISF (55 %). Likewise, in the Fe_3O_4 nano systems (Mode SNLISF, 58 %; Mode SLNISF, 59 %; Mode NSLISF, 55 %), aliphatic acids concentrations were lower when compared to the control set-up (69 %). This suggests metabolic shift away from ethanol production in the control set-up towards organic acid formation, especially acetic acid formation (Table 4), while the opposite can be suggested for the nano-administered processes. The formation of less acetic acid is of benefit to ethanol production by *S. cerevisiae* [28]. This agrees with the observation in this study, where higher bioethanol concentrations were associated with the NIISF processes, which had lesser acetic acid concentrations when compared to the control experiment (ISF without nanoparticles). Cellular accumulation of acetic acid is detrimental to the cell and the overall fermentation process performance. Also, notable is the lowest acid concentration (55 %) obtained in Mode NSLISF of both nano systems, suggesting the stage of NPs inclusion was vital to its impact on the acid inhibitor formation. Furthermore, in this study, high ethanol yield (>0.93 g/g), lower concentration of aliphatic acids (<69 %), benzenoids (<7 %), lactones (<0.08 %), sulphur-containing compounds (<0.35 %), phenolics (<0.08 %) and alkanal (<0.08 %) were associated with nano supplementation. The distribution of metabolites formed during ethanol production is a crucial signal in assessing the efficiency of the process [43]. To maximise the yield of ethanol, the metabolic activities (by *S. cerevisiae*) must be directed away from these volatile organic inhibitory compounds. In this study, the shift in metabolic pathway away from volatile organic inhibitory compound formation, towards ethanol production can be ascribed to the presence of nanobiocatalyst [62]. Noticeable is the disparity in the concentrations of VOIcs obtained in the nano-administered processes and the control experiments. For instance, lower concentrations of acetic acid (<7.837 g/L) and levulinic acid (<0.104 g/L) were observed in the nano system as against the control experiments (>16.073, >0.162 g/L, respectively), representing a 105 % and 56 % reduction in acetic and levulinic acid respectively in the nano system. Similarly ketone, such as 1-Hydroxy-2-propanone (<0.055 g/L), was in lesser concentration in comparison to the control experiments (0.063 g/L), also representing a 15 % reduction in 1-Hydroxy-2-propanone concentration in the nano system. Furthermore, the sulphur compound, dimethyl trisulfide was 7.9-fold less in the nano systems in comparison to the control set-up. These results further vindicate the inclusion of nanoparticles in the ISF process.

Table 4
Relative amounts (g/L) of volatile organic inhibitory compounds from ISF processes with nanoparticle (NiO and Fe_3O_4) inclusion.

Compounds	NiO NPs ISF						Fe_3O_4 NPs ISF					
	1	2	3	4	5	6	1	2	3	4	5	6
Amines												
3-methyl-pyridine	0.022	0.026	0	0.010	0.013	0	0	0	0	0	0	0
Amides												
Acetamide	0	0	0	0	0	0.032	0	0	0	0	0	0
Alcohols												
3-Methyl-1-butanol	0.152	0.123	0.295	0.177	0.026	0	0	0.081	0.090	0.167	0	0
Pentanol	0	0	0	0	0	0	0.054	0	0	0	0	0
2,3-Butanediol	0	0	0	0	0	0	0	0	0	0	0	0
2-Furanmethanol	0.293	0.125	0.114	0.203	0.105	1.137	0.105	0.076	0.151	0.141	0.210	0.598
5-Methyl-2-furanmethanol	0.059	0.020	0	0.062	0.071	0.226	0.059	0.033	0.049	0.046	0.044	0.192
3-(methylthio)-1-Propanol	0.056	0.047	0.090	0.053	0.047	0	0.060	0.057	0.045	0.082	0	0
2-Methoxy phenol	0.055	0	0.018	0	0.092	0	0	0	0	0	0	0
Phenylethyl Alcohol	0.602	0.422	0.375	0.582	0.292	0	0.374	0.498	0.353	0.667	0	0
Benzyl alcohol	0	0	0	0	0	0.297	0.026	0	0	0		0
4-hydroxy-benzenemethanol	0	0	0	0	0	0.061	0	0	0	0	0.026	0.055
Cinnamyl alcohol	0.092	0	0.128	0.099	0.098	0	0	0	0	0	0	0.019
1-(2-Furyl)-,2-ethanediol	1.559	1.138	1.223	1.672	0.919	0.164	1.002	1.567	0.825	1.657	0.085	0.072
Aldehydes												
Fufural	0.098	0.098	0.107	0.228	0	2.798	0.150	0.083	0.098	0.152	0.726	1.808
5-Methyl-fufural	0.263	0.278	0	0.307	0.220	3.367	0.348	0.323	0.352	0.406	0.387	1.427
5-Hydroxymethylfufural	0	0	0	0	0.054	5.844	0	0	0	0	2.509	4.781
Aliphatic acids												
Acetic acid	7.837	7.187	16.073	7.642	2.464	7.220	6.032	6.966	7.016	7.416	1.171	4.573
Formic acid	0	0	0.127	0.022	0	0	0	0	0.043	0	0.020	0.148
Propanoic acid	0.090	0.064	0.162	0.111	0.044	0	0	0.103	0	0.170	0.023	0.038
Isobutyric acid	0.077	0.064	0.133	0.071	0	0	0.111	0.083	0.053	0.075	0.031	0.048
4-Hydroxybutanoic acid	0	0	0	0	0	0	0.084	0.174	0.084	0	0.026	0.077
Butanoic acid	0.055	0.046	0	0.091	0.320	0	0	0	0	0.083	0.026	0
Isovaleric acid	0	0	0	0	0	0	0.061	0	0	0	0	0
2-Methylhexanoic acid	0.064	0.036	0.165	0.095	0.059	0	0	0.067	0.049	0.076	0	0
Valeric acid	0	0	0	0	0	0	0	0	0.070	0	0	0
Hexanoic acid	0.059	0.057	0.086	0.090	0.051	0	0.071	0.076	0.056	0.104	0.053	0.098
Larixinic acid	0.063	0.062	0.198	0.082	0.059	0.084	0.075	0.068	0.075	0.090	0.013	0.065
Sorbic acid	0.116	0.151	0	0.171	0.046	0	0.070	0.123	0.054	0.202	0.036	0.198
Octanoic acid	0	0	0	0	0	0	0	0	0	0	0.083	0.052
Levulinic acid	0.078	0.097	0.162	0	0.031	0.081	0.076	0.095	0.100	0.104	0.042	0.043
Benzenoids												
Benzeneacetaldehyde	0.461	0.371	1.283	0.733	0.344	0.815	0.587	0.446	0.389	0.581	0.030	0.393
Benzoic acid	0	0.155	0.497	0	0	0	0	0.175	0.119	0.185	0.061	0.206
Ketones												
Acetoin	0	0	0	0	0.187	0	0	0	0	0	0	0
1-Hydroxy-2-propanone	0.034	0.037	0.043	0.028	0.051	0.213	0.055	0.048	0.063	0.027	0.076	0.133
Ethenone, 1-(2-furanyl)	0	0	0.485	0.087	0.033	0.138	0	0	0	0.065	0.035	0.186
2-Pyrrolidinone	0.051	0.039	0.071	0.058	0.022	0	0.041	0.045	0.040	0.049	0	0
Ethenone	0.198	0.140	0.268	0.255	0.130	0.158	0.136	0.173	0.145	0.207	0.054	0.061
Furyl hydroxymethyl ketone	0	0	0	0	0	0.116	0	0	0	0	0.019	0.051
2,5-Dimethyl-4-hydroxy-3(2 H)-furanone	0.242	0.260	0.555	0.339	0.140	0.247	0.247	0.223	0.200	0.315	0.105	0.144
2,3-dihydro-3,5-dihydroxy-6-methyl-4H-Pyran-4-one	1.595	1.271	1.815	1.956	1.538	7.601	1.391	1.562	1.397	2.034	4.649	6.170
4-cyclopenetene-1,3-dione	0	0	0	0	0	0	0	0	0	0	0.082	0.169
Lactones												
5-Methyl-2(5 H)-Furanone	0	0	0	0	0	0	0	0	0	0	0	0.026
2(5 H)-Furanone	0	0	0	0	0	0	0	0.008	0.010	0	0.014	0.038
Sulphur compounds												
Dimethyl disulphide	0	0	0	0	0	0	0	0	0	0	0	0.031
Dimethyl trisulfide	0.009	0.007	0.087	0.011	0	0	0	0.007	0.009	0.011	0	0
Phenolic compounds												
2-Methoxy phenol	0.055	0	0.018	0	0.092	0	0	0	0	0	0	0
2-Methoxy-4-vinylphenol	0.084	0.073	0.172	0.100	0.017	0.180	0.062	0.076	0.063	0.139	0.019	0.110
Alkanal												
Methional	0	0	0	0	0	0.129	0	0	0.009	0.011	0	0

1- SNLISF, 2-SLNISF, 3-SLISF-control, 4-NSLISF, 5-SLIS and 6-NSLIS.

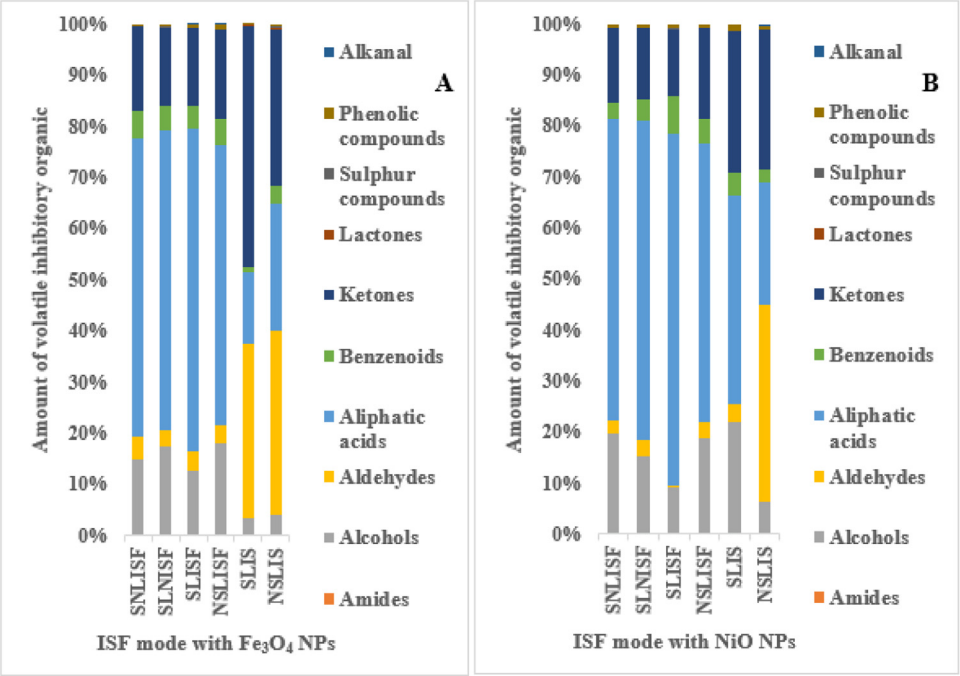

Fig. 8. Profile of volatile organic inhibitory compounds in different modes of ISF processes in the presence of nanocatalysts (A) Fe_3O_4 NPs and (B) NiO NPs.

3.6. Effects of stage of nanoparticle inclusion in the ISF inhibitor compounds profile

There were differences in the concentrations of bioethanol and volatile organic compounds observed in the NIISF processes resulting from the different stages of nanoparticle inclusion in the ISF processes. Inclusion of NiO NPs at the pre-treatment stage (Mode NSLISF), suggests an improved alcoholic metabolic pathway resulting in the highest bioethanol concentration of 36.04 g/L and considerable reduction in acetic acid formation (27 %). The results obtained with NPs administered at the liquefaction, saccharification and fermentation stages (Modes SNLISF and SLNISF) indicate the enzymatic and yeast metabolic activities were shifted away from sulphur-containing and phenolic compound formation. Also, the acetic acid was reduced by administering NPs at these stages, but to a lesser extent (10 %). The impact of nanoparticles on volatile inhibitory compound formation may be ascribed to the protonation degradation of potato peel biomass during the physiochemical pre-treatment process and the enzymatic activities during the NIISF processes [51]. Protonation site initiating substrate degradation determines the mechanism and degradation pathway, consequently, the degradation products [61]. Similarly, the degradation products depend on operating conditions and could be regulated by controlling the process parameters. In addition, the formation of organic metabolites also occasion by the amounts of enzymes and co-factors such as nickel and iron present, thus, from enzyme regulatory mechanisms, and the need to maintain a relatively steady intracellular pH [63]. Inclusion of metallic supplement in bioprocessing performs various functions such as enzyme activator, enzymes stabilisers, enzymes cofactor, growth factor and chelating of other compounds hence, reducing their toxicity [57]. Moreover, volatile organic inhibitory compounds (VOIcs) released due to substrate metabolism have chelating potentials and capacities occasioned by their functional groups [64]. These chelating compounds such as sulfhydryls, amides, carboxylates, hydroxyls, phenols and amines can form ligands and complexes with Fe and Ni metals. The affinity for complexation with VOIcs and subsequent bioavailability of these metals are not the same for various metals; and this is also dependent on operating conditions [27]. Consequently, the VOIcs formed, and their chelating activities in bioprocesses play vital roles in metal ions' availability to microorganisms, metabolic activities and ultimately process performance.

4. Conclusions

The impact of inclusion stage of NiO and Fe_3O_4 nanoparticles on bioethanol production and volatile inhibitory organic compound formation in the instantaneous saccharification and fermentation (ISF) of potato peels is elucidated in detail. Addition of NiO NPs at the pre-treatment stage (NSLISF mode) resulted in the production of optimal concentration of bioethanol (36.04 g/L). Likewise, inclusion of Fe_3O_4 NPs during pre-treatment (NSLISCF) and liquefaction (SNLISF) stages lead to the best bioethanol concentration values of 23.99 and 23.75 g/L respectively. Higher ethanol yield (0.93 g/g) with inclusion of Fe_3O_4 NPs during liquefaction and productivity (2.25 g/L/h) with inclusion of NiO NPs during pre-treatment were obtained with the NIISF processes. Moreover, substantial reduction in inhibitory organic compounds was also achieved with the NIISF (nanoparticle inclusion) strategy. Nanoparticle band gap energy property had a pronounced effect on bioethanol bioprocessing. These nano additives are effective biocatalysts; their individual inclusion had significant impact on the biomass conversion processes (pre-treatment, liquefaction, saccharification and fermentation). Hence, NiO and Fe_3O_4 nanoparticles could be an efficient biocatalyst for the industrial bioethanol production from potato peels.

Author contributions

The experiment conceptualization was conceived and designed by Isaac A. Sanusi and Gueguim EB. Kana; experimental investigation and data curation were conducted by Isaac A. Sanusi, while, Terence N. Suinyuy conducted investigation on volatile inhibitory compounds. Isaac A. Sanusi wrote the manuscript for publication under the supervision of Gueguim EB. Kana.

Declaration of Competing Interest

The authors report no declarations of interest.

References

[1] L.J. Jönsson, C. Martín, Pre-treatment of lignocellulose: formation of inhibitory by-products and strategies for minimizing their effects, Bioresour. Technol. 199 (2016) 103–112, doi:http://dx.doi.org/10.1016/j.biortech.2015.10.009.

[2] U. Talasila, R.R. Vechalapu, Optimization of medium constituents for the production of bioethanol from cashew apple juice using doehlert experimental design, Int. J. Fruit Sci. 15 (2015) 161–172, doi:http://dx.doi.org/10.1080/15538362.2014.989134.

[3] S. Shanavas, G. Padmaja, S.N. Moorthy, M.S. Sajeev, J.T. Sheriff, Process optimization for bioethanol production from cassava starch using novel eco-friendly enzymes, Biomass Bioenergy 35 (2011) 901–909, doi:http://dx.doi.org/10.1016/j.biombioe.2010.11.004.

[4] M. Puri, R.E. Abraham, C.J. Barrow, Biofuel production: prospects, challenges and feedstock in Australia, Renew. Sustain. Energy Rev. 16 (2012) 6022–6031, doi:http://dx.doi.org/10.1016/j.rser.2012.06.025.

[5] C.N. Ncobela, A.T. Kanengoni, V.A. Hlatini, R.S. Thomas, M. Chimonyo, A review of the utility of potato by-products as a feed resource for smallholder pig production, Anim. Feed Sci. Technol. 227 (2017) 107–117, doi:http://dx.doi.org/10.1016/j.anifeedsci.2017.02.008.

[6] A.F.S. Maldonado, E. Mudge, M.G. Gänzle, A. Schieber, Extraction and fractionation of phenolic acids and glycoalkaloids from potato peels using acidified water/ethanol-based solvents, Food Res. Int. 65 (2014) 27–34, doi:http://dx.doi.org/10.1016/j.foodres.2014.06.018.

[7] M. Kim, J. Kim, Comparison through a LCA evaluation analysis of food waste disposal options from the perspective of global warming and resource recovery, Sci. Total Environ. 408 (2010) 3998–4006, doi:http://dx.doi.org/10.1016/j.scitotenv.2010.04.049.

[8] D. Arapoglou, T.H. Varzakas, A. Vlyssides, C. Israilides, Ethanol production from potato peel waste (PPW), Waste Manag. 30 (2010) 1898–1902, doi:http://dx.doi.org/10.1016/j.wasman.2010.04.017.

[9] M. Lech, Optimisation of protein-free waste whey supplementation used for the industrial microbiological production of lactic acid, Biochem. Eng. J. 157 (2020) 107531, doi:http://dx.doi.org/10.1016/j.bej.2020.107531.

[10] A. Kristiani, H. Abimanyu, A.H.S. Sudiyarmanto, F. Aulia, Effect of pretreatment process by using diluted acid to characteristic of oil palm's frond, Energy Procedia 32 (2013) 183–189, doi:http://dx.doi.org/10.1016/j.egypro.2013.05.024.

[11] J. Mäder, H. Rawel, L.W. Kroh, Composition of phenolic compounds and glycoalkaloids α-solanine and α-chaconine during commercial potato processing, J. Agric. Food Chem. 57 (2009) 6292–6297, doi:http://dx.doi.org/10.1021/jf901066k.

[12] M.S. Hashem, M.I. Darwish, Production of bioethanol and associated by-products from potato starch residue stream by *Saccharomyces cerevisiae*, Biomass Bioenergy 34 (2010) 953–959, doi:http://dx.doi.org/10.1016/j.biombioe.2010.02.003.

[13] G. Izmirlioglu, A. Demirci, Ethanol production from waste potato mash by using *Saccharomyces cerevisiae*, Appl. Sci. 2 (2012) 738–753, doi:http://dx.doi.org/10.3390/app2040738.

[14] B.J. Khawla, M. Sameh, G. Imen, F. Donyes, G. Dhouha, E.G. Raoudha, N.-E. Oumèma, Potato peel as feedstock for bioethanol production: a comparison of acidic and enzymatic hydrolysis, Ind. Crops Prod. 52 (2014) 144–149, doi:http://dx.doi.org/10.1016/j.indcrop.2013.10.025.

[15] M. Fadel, Alcohol production from potato industry starchy waste, Egypt J. Microbiol. 35 (2000) 273–287 ISSN: 0022-2704.

[16] Y. Sewsynker-Sukai, E.B. Gueguim Kana, Simultaneous saccharification and bioethanol production from corn cobs: process optimization and kinetic studies, Bioresour. Technol. 262 (2011) 32–41, doi:http://dx.doi.org/10.1016/j.biortech.2018.04.056.

[17] P. Ariyajaroenwong, P. Laopaiboon, A. Salakkam, P. Srinophakun, L. Laopaiboon, Kinetic models for batch and continuous ethanol fermentation from sweet sorghum juice by yeast immobilized on sweet sorghum stalks, J. Taiwan Inst. Chem. Eng. 66 (2016) 210–216, doi:http://dx.doi.org/10.1016/j.jtice.2016.06.023.

[18] K. Doriya, D.S. Kumar, Solid state fermentation of mixed substrate for l-asparaginase production using tray and in-house designed rotary bioreactor, Biochem. Eng. J. 138 (2018) 188–196, doi:http://dx.doi.org/10.1016/j.bej.2018.07.024.

[19] J.M. Dodic, D.G. Vucurovic, S.N. Dodic, J.A. Grahovac, S.D. Popov, N.M. Nedeljković, Kinetic modelling of batch ethanol production from sugar beet raw juice, Appl. Energy 99 (2012) 192–197, doi:http://dx.doi.org/10.1016/j.apenergy.2012.05.016.

[20] N. Phukoetphim, A. Salakkam, P. Laopaiboon, L. Laopaiboon, Kinetic models for batch ethanol production from sweet sorghum juice under normal and high gravity fermentations: logistic and modified Gompertz models, J. Biotech 243 (2017) 69–75, doi:http://dx.doi.org/10.1016/j.jbiotec.2016.12.012.

[21] E. Abdelsalam, M. Samer, Y.A. Attia, M.A. Abdel-Hadi, H.E. Hassan, Y. Badr, Comparison of nanoparticles effects on biogas and methane production from anaerobic digestion of cattle dung slurry, Renew. Energy 87 (2016) 592–598, doi:http://dx.doi.org/10.1016/j.renene.2015.10.053.

[22] P.T. Sekoai, C.N.M. Ouma, S.P. du Preez, P. Modisha, N. Engelbrecht, D.G. Bessarabov, A. Ghimire, Application of nanoparticles in biofuels: an overview, Fuel 237 (2019) 380–397, doi:http://dx.doi.org/10.1016/j.fuel.2018.10.030.

[23] E. Cherian, M. Dharmendirakumar, G. Baskar, Immobilization of cellulase onto MnO_2 nanoparticles for bioethanol production by enhanced hydrolysis of agricultural waste, Chin. J. Catal. 35 (2015) 1223–1229, doi:http://dx.doi.org/10.1016/S1872-2067(15)60906-8.

[24] A.I. Sanusi, F.D. Faloye, E.B. Gueguim Kana, Impact of various metallic oxide nanoparticles on ethanol production by *Saccharomyces cerevisiae* BY4743: screening, kinetic study and validation on potato waste, Catal. Lett. 149 (7) (2019) 2015–2031, doi:http://dx.doi.org/10.1007/s10562-019-02796-6.

[25] D.K. Ban, S. Paul, Zinc oxide nanoparticles modulates the production of β-Glucosidase and protects its functional state under alcoholic condition in *Saccharomyces cerevisiae*, Appl. Biochem. Biotechnol. 173 (2014) 155–166, doi:http://dx.doi.org/10.1007/s12010-014-0825-2.

[26] Y. Kim, H. Lee, Use of magnetic nanoparticles to enhance bioethanol production in syngas fermentation, Bioresour. Technol. 204 (2016) 139–144, doi:http://dx.doi.org/10.1016/j.biortech.2016.01.001.

[27] P.M. Thanh, B. Ketheesan, Z. Yan, D. Stuckey, Trace metal speciation and bioavailability in anaerobic digestion: a review, Biotechnol. Adv. 34 (2016) 122–136, doi:http://dx.doi.org/10.1016/j.biotechadv.2015.12.006.

[28] H. Han, M. Cui, L. Wei, H. Yang, J. Shen, Enhancement effect of hematite nanoparticles on fermentative hydrogen production, Bioresour. Technol. 102 (2011) 7903–7909, doi:http://dx.doi.org/10.1016/j.biortech.2011.05.089.

[29] A. Cavka, L.J. Jönsson, Detoxification of lignocellulosic hydrolysates using sodium borohydride, Bioresour. Technol. 136 (2013) 368–376, doi:http://dx.doi.org/10.1016/j.biortech.2013.03.014.

[30] D.C.S. Rorke, T.N. Suinyuy, E.B. Gueguim Kana, Microwave-assisted chemical pre-treatment of waste sorghum leaves: process optimization and development of an intelligent model for determination of volatile compound fractions, Bioresour. Technol. 224 (2017) 590–600, doi:http://dx.doi.org/10.1016/j.biortech.2016.10.048.

[31] N. Cheng, K. Koda, Y. Tamai, Y. Yamamoto, T.E. Takasuka, Y. Uraki, Optimization of simultaneous saccharification and fermentation conditions with amphipathic lignin derivatives for concentrated bioethanol production, Bioresour. Technol. 232 (2017) 126–132, doi:http://dx.doi.org/10.1016/j.biortech.2017.02.018.

[32] Y. Kim, S.E. Park, H. Lee, J.Y. Yun, Enhancement of bioethanol production in syngas fermentation with *Clostridium ljungdahii*using nanoparticles, Bioresour. Technol. 159 (2014) 446–450, doi:http://dx.doi.org/10.1016/j.biortech.2014.03.046.

[33] A.I. Sanusi, T.N. Suinyuy, A. Lateef, E.A. Gueguim Kana, Effect of nickel oxide nanoparticles on bioethanol production: process optimization, kinetic and metabolic studies, Process. Biochem. 92 (2020) 386–400, doi:http://dx.doi.org/10.1016/j.procbio.2020.01.029.

[34] J.B. Sluiter, R.O. Ruiz, C.J. Scarlata, A.D. Sluiter, D.W. Templeton, Compositional analysis of lignocellulosic feedstocks. 1. Review and description of methods, J. Agric. Food Chem. 58 (16) (2010) 9043–9053, doi:http://dx.doi.org/10.1021/jf1008023.

[35] G.S. Aruwajoye, F.D. Faloye, E.B. Gueguim Kana, Soaking assisted thermal pre-treatment of cassava peels wastes for fermentable sugar production: process modelling and optimization, Energy Convers. Manage. 150 (2017), doi:http://dx.doi.org/10.1016/j.ijhydene.2014.01.163 558–56.

[36] G. Prochazkova, I. Safarik, T. Branyik, Harsvesting microalgae with microwave synthesized magnetic microparticles, Bioresour. Technol. 130 (2013) 472–477, doi:http://dx.doi.org/10.1016/j.biortech.2012.12.060.

[37] Ritu, Synthesis and characterization of chromium oxide nanoparticles, IOSR J. Appl. Chem. (IOSR-JAC) 8 (3) (2015) 05–11, doi:http://dx.doi.org/10.9790/5736-08310511 Ver. I.

[38] D.K. Vizhi, N. Supraja, A. Devipriya, N.V.K.V.P. Tollamadugu, R. Babujanarthanam, Evaluation of antibacterial activity and cytotoxic effects of green AgNPs against breast cancer cells (MCF 7), Adv. Nano Res. 4 (2) (2016) 129–143.

[39] M. El-Kemary, N. Nagy, I. El-Mehasseb, Nickel oxide nanoparticles: synthesis and spectral studies of interactions with glucose, Mater. Sci. Semicond. Process. 16 (2013) 1747–1752, doi:http://dx.doi.org/10.1016/j.mssp.2013.05.018.

[40] B. Sawicki, E. Tomaszewicz, M. Piątkowska, T. Groń, H. Duda, K. Górny, Correlation between the band-gap energy and the electrical conductivity in $MPr_2W_2O_{10}$ tungstates (Where m = Cd, Co, Mn), Acta Phys. Pol. A 129 (No. 1-A) (2016), doi:http://dx.doi.org/10.12693/APhysPolA.129.A-94.

[41] A. Mondal, A. Mondal, D. Mukherjee, Room-temperature synthesis of cobalt nanoparticles and their use as catalysts for Methylene Blue and Rhodamine-B dye degradation, Adv. Nano Res. 3 (2) (2015) 67–79, doi:http://dx.doi.org/10.12989/anr.2015.3.2.067.

[42] Y.Y. Choong, I. Norli, A.Z. Abdullah, M.F. Yhaya, Impacts of trace element supplementation on the performance of anaerobic digestion process: a critical review, Bioresour. Technol. 209 (2016) 369–379, doi:http://dx.doi.org/10.1016/j.biortech.2016.03.028.

[43] Y. Zhang, J. Shen, Enhancement effect of gold nanoparticles on biohydrogen production from artificial wastewater, Int. J. Hydrogen Energy 32 (1) (2007) 17–23, doi:http://dx.doi.org/10.1016/j.ijhydene.2006.06.004.

[44] S.K. Lower, M.F. Hochella Jr, T.J. Beveridge, Bacterial recognition of mineral surfaces: nanoscale interactions between *Shewanella* and a-FeOOH, Science 292 (5520) (2001) 1360–1363, doi:http://dx.doi.org/10.1126/science.1059567.

[45] A. Verma, F. Stellacci, Effect of surface properties on nanoparticle–cell interactions, Small 6 (1) (2010) 2–21, doi:http://dx.doi.org/10.1002/smll.200901158.
[46] S. Faramarzi, Y. Anzabi, H. Fararizadeh-Malmiri, Selenium supplementation during fermentation with sugar beet molasses and *saccharomyces cerevisiae* to increase bioethanol production, Green Process. Synth. 8 (1) (2019) 622–628, doi:http://dx.doi.org/10.1515/gps-2019-0032.
[47] G. Izmirlioglu, A. Demirci, Improved simultaneous saccharification and fermentation of bioethanol from industrial potato waste with co-cultures of *Aspergillus niger* and *Saccharomyces cerevisiae* by medium optimization, Fuel 185 (2016) 684–691, doi:http://dx.doi.org/10.1016/j.fuel.2016.08.035.
[48] P. Moodley, E.B. Gueguim Kana, Bioethanol production from sugarcane leaf waste: effect of various optimized pre-treatments and fermentation conditions on process kinetics, Biotechnol. Rep. 24 (2019) 1–8, doi:http://dx.doi.org/10.1016/j.btre.2019.e00329.
[49] S. Kodhaiyolii, S.R. Mohanraj, M. Engasamy, V. Pugalenthi, Phytofabrication of bimetallic Co-Ni nanoparticles using Boerhavia diffuse leaf extract: analysis of phytocompounds and application for simultaneous production of biohydrogen and bioethanol, Mater. Res. Express 6 (9) (2019). https://iopscience.iop.org/article/10.1088/2053-1591/ab2ea8/meta.
[50] A. Kumar, S. Singh, R. Tiwar, R. Goel, L. Nain, Immobilization of indigenous holocellulase on iron oxide (Fe_2O_3) nanoparticles enhanced hydrolysis of alkali pre-treated paddy straw, Int. J. Biol. Macromol. 96 (2017) 538–549.
[51] N. Dutta, M.K. Saha, Nanoparticle-induced enzyme pre-treatment method for increased glucose production from lignocellulosic biomass under cold conditions, J. Sci. Food Agric. 99 (2) (2019) 767–780, doi:http://dx.doi.org/10.1002/jsfa.9245.
[52] M. Rai, A.P. Ingle, R. Pandit, J.K.Biswas Paralikar, S.S. da Silva, Emerging role of nanobiocatalysts in hydrolysis of lignocellulosic biomass leading to sustainable bioethanol production, Catal. Rev.-Sci. Eng. 61 (1) (2019) 1–26, doi:http://dx.doi.org/10.1080/01614940.2018.1479503.
[53] Z.C. Gou, N.L. Ma, W.Q. Zhang, Z.P. Lei, Y.J. Su, C.Y. Sun, G.Y. Wang, H. Chen, S.T. Zhang, G. Chen, Y. Sun, Innovative hydrolysis of corn stover bio waste by modified magnetite laccase immobilized nanoparticles, Environ. Res. 188 (2020).
[54] S. Chamoli, E. Yadav, J.K. Saini, A.K. Verma, N.K. Navani, P. Kumar, Magnetically recyclable catalytic nanoparticles grafted with *Bacillus subtilis* beta-glucosidase for efficient cellobiose hydrolysis, Int. J. Biol. Macromol. 164 (2020) 1729–1736, doi:http://dx.doi.org/10.1016/j.ijbiomac.2020.08.102.
[55] A.I. Sanusi, T.N. Suinyuy, A. Lateef, E.B. Gueguim Kana, Effect of nickel oxide nanoparticles on bioethanol production: process optimization, kinetic and metabolic studies, Process. Biochem. 92 (2020) 386–400, doi:http://dx.doi.org/10.1016/j.procbio.2020.01.029.
[56] J.L. Linville, M. Rodriguez Jr, J.R. Mielenz, C.D. Cox, Kinetic modeling of batch fermentation for Populus hydrolysate tolerant mutant and wild type strains of *Clostridium thermocellum*, Bioresour. Technol. 147 (2013) 605–613, doi:http://dx.doi.org/10.1016/j.biortech.2013.08.086.
[57] A. Schattauer, E. Abdoun, P. Weiland, M. Plöch, M. Heiermann, Abundance of trace elements in demonstration biogas plants, Biosyst. Eng. 108 (2011) 57–65, doi:http://dx.doi.org/10.1016/j.biosystemseng.2010.10.010.
[58] T. Srimachai, K. Nuithitikul, S. O-thong, P. Kongjan, K. Panpong, Optimization and kinetic modeling of ethanol production from oil palm frond juice in batch fermentation, Energy Procedia 79 (2015) 111–118, doi:http://dx.doi.org/10.1016/j.egypro.2015.11.490.
[59] D.C.S. Rorke, E.B. Gueguim Kana, Kinetics of bioethanol production from waste sorghum leaves using *Saccharomyces cerevisiae* BY4743, Fermentation 3 (2017) 19, doi:http://dx.doi.org/10.3390/fermentation3020019.
[60] Y.P. Teoh, M.M. Don, S. Ujang, Media and antifungal activity, BioResources 6 (3) (2011) 2719–2731.
[61] H. Rasmussen, H.R. Sørensen, A.S. Meyer, Formation of degradation compounds from lignocellulosic biomass in the biorefinery: sugar reaction mechanisms, Carbohydr. Res. 385 (2014) 45–57, doi:http://dx.doi.org/10.1016/j.carres.2013.08.029.
[62] P. Wimonsong, R. Nitisoravut, Comparison of different catalysts for fermentative hydrogen production, J. Clean Energy Technol. 3 (2) (2015) 128–131, doi:http://dx.doi.org/10.7763/JOCET.2015.V3.181.
[63] K.G. Mackenzie, M.C. Kenny, Non-volatile organic acid and pH changes during the fermentation of distiller's wort, J. Inst. Brew. (1985) 71, doi:http://dx.doi.org/10.1002/j.2050-0416.1965.tb02040.x.
[64] W.-C. Kuo, G.F. Parkin, Characterization of soluble microbial products from anaerobic treatment by molecular weight distribution and nickel-chelating properties, Water Res. 30 (1996) 915–922, doi:http://dx.doi.org/10.1016/0043-1354(95)00201-4.